JOURNAL OF PROPULSION AND POWER
Vol. 13, No. 3, May–June 1997

Modular Prediction Scheme for Blade Row Interaction Noise

A. B. Parry*
Rolls–Royce, plc., Derby DE24 8BJ, England, United Kingdom

A previously developed method for the prediction of contrarotating propeller noise is extended, with minimal modification, for application to many-bladed configurations. The resultant scheme is applied to rotor–stator, stator–rotor, and rotor–rotor aerodynamic interactions on ducted rotors. Two classical wake models and a semiempirical wake model are considered; these models are compared with wake data from a fan rig, and it is shown that the classical models are far superior to the semiempirical model. Far-field predictions of sound power (neglecting blade row attenuation) are compared with measured data from a conventional single-stream fan rig and from a contrarotating ducted fan model. Theory and noise data are shown to agree reasonably well for both sets of data and at all frequencies, without taking any account of rotor blockage. The results suggest that the level of agreement could be improved further by some modifications to the wake model and by the inclusion of rotor blockage effects in the prediction scheme.

Nomenclature

b = wake width (measured normal to the mean flow direction)
C_D = blade section drag coefficient
$C(z)$ = $\int_0^z \cos(\pi t^2/2)\, dt$ is the Fresnel cosine integral
c = blade section chord
E = shaft frequency
G = normalized Fourier coefficient
k = integer
k_b = wake wave number
m = mode number
n = harmonic
s = blade pitch
U_∞ = mean relative flow speed
u = wake defect velocity
(X, Y) = coordinates measured parallel and normal to the wake centerline
(x, y) = coordinates measured parallel and normal to the engine axis
α = blade exit flow angle

Subscripts
1/2 = at half the wake centerline defect velocity
0 = at blade trailing edge
1, 2 = front, rear blade rows

I. Introduction

IN recent years good progress has been made in the prediction of noise radiated from contrarotating propellers (CRPs), these prediction schemes being not just empirical but analytical in nature and capable of predicting both absolute levels, rather than just trends in the data, and also precise features of the radiated directivity. However, similar progress has not, in general, been made in the (analytical) prediction of fan noise, although some advances in this direction have been made by Topol.[1] Certainly the main tonal noise generating mechanisms are the same on both CRPs and fans, i.e., aerodynamic interactions, both wake and potential, between blade rows. However, there is one additional feature present in fan noise, namely noise propagation effects, such as propagation through a blade row.

A modular approach, which can be used to predict (far-field) noise radiated from propfans, contrafans, and turbofans with separate modules for the unsteady velocity fields, the unsteady blade row response, and the sound radiation, is described in this paper. The prediction scheme is purely analytical, based on developments to an original propfan prediction scheme.[2] In this study attention is restricted to aerodynamic interactions between blade rows (rotor–stator, stator–rotor, or rotor–rotor) and the resultant sound radiated to the far field. Consequently, the interactions between incident steady or unsteady distortion and a rotor, and also blade row transmission effects are neglected. However, it is emphasized that these effects, and others, can be incorporated into the general framework and, indeed, relevant frequency domain schemes for distortion rotor interaction and three-dimensional effects in gust-blade row interactions have been published[3,4] and a detailed description of a scheme for sound propagation through a blade row, which is compatible with the general scheme described here and represents a propagation module, will be published by the present author elsewhere. Note, also, that a very general overview of the framework, showing how other fan noise generation and propagation mechanisms can be included in the scheme, is given by Crighton.[5]

Section II has a description of the viscous wake velocity fields and their decomposition into Fourier harmonics. Three wake models are considered, a semiempirical model and two classical models, and comparisons are shown between the models and measured wake data. The open rotor blade response calculations are described in Sec. III where we outline the extensions to the propfan unsteady response approach that are necessary for application to many-bladed fans. Radiation of the sound, generated by the unsteady blade forces, to the far field is discussed in Sec. IV. Finally, comparisons of predictions with data from a contrarotating ducted fan rig and from a conventional single-stream fan rig are discussed in Sec. V, along with a discussion of previous comparisons between the method and data from flight tests on a contrarotating propeller. The comparisons are used to select the best of the three wake models and, for that model, to show its range of validity and to suggest further improvements that could be made to the model. In addition, the results for far-field noise are used to assess any limitations of the prediction scheme used here, and additional modules that could be included to enhance the level of agreement between theory and data.

Presented as Paper 95-024 at the CEAS/AIAA 1st Joint Aeroacoustics Conference, Munich, Germany, June 12–15, 1995; received Aug. 19, 1996; revision received Dec. 4, 1996; accepted for publication Dec. 18, 1996.

*Staff Technologist, Aerothermal Methods Group, P.O. Box 31.

The intention is to show how relatively simple analytical methods can be used to construct an efficient robust method that is easy to use, particularly at the preliminary design stage for the accurate prediction of aerodynamic interaction noise in the far field, and that a single method can be applied to open or ducted rotors, and to rotor–stator, rotor–rotor, or stator–rotor interactions.

II. Wake Profiles and Harmonics

A. Models

Two standard and classical models for wake development are considered first. These models can be derived analytically using two slightly different versions of Prandtl's mixing length theory described in, for example, Chap. 14 of Schlichting[6] or Chap. 5 of Goldstein.[7] In both cases the wakes are assumed to be two dimensional and to conserve momentum.

The first model is referred to here as the Schlichting wake model,[8] and its derivation is described in detail in Chap. 13 of Goldstein[7] and Chap. 24 of Schlichting.[6] The fractional velocity deficit is given by

$$\frac{u}{U_\infty} = \frac{\sqrt{10}}{18\beta}\left(\frac{C_D}{X/c}\right)^{1/2}\left(1 - \left|\frac{Y}{b}\right|^{3/2}\right)^2 \tag{1}$$

Note that the usual approach is to take X as measured from a virtual source position inside the blade trailing edge. The corresponding wake semiwidth, which together with Eq. (1) satisfies conservation of momentum, is

$$b/c = \beta\sqrt{10}C_D^{1/2}(X/c)^{1/2} \tag{2}$$

where the parameter β, used in both Eqs. (1) and (2), needs to be determined empirically. Experiments carried out by Schlichting[8] and Reichardt[9] on circular cylinders of different diameters, suggested that the half-wake semiwidth $b_{1/2}$, defined at half the centerline defect velocity, varies with X according to

$$b_{1/2}/c = \tfrac{1}{4}C_D^{1/2}(X/c)^{1/2} \tag{3}$$

which results in the value $\beta = 0.18$.

A number of authors used a Gaussian profile to represent the wake. The classical model used here and referred to as the Reichardt wake model[9,10] is described in Chap. 24 of Schlichting.[6] The fractional velocity deficit is given as

$$\frac{u}{U_\infty} = \frac{C_D^{1/2}}{4\sqrt{\pi}}(cC_DU_\infty/\varepsilon)^{1/2}(X/c)^{-1/2}\exp\left[-\frac{cC_DU_\infty/\varepsilon}{4C_D(X/c)}\frac{Y^2}{c^2}\right] \tag{4}$$

where ε is an empirically determined constant. By using Eq. (3), along with conservation of momentum, we obtain

$$cC_DU_\infty/\varepsilon = 64\ \log\ 2 \tag{5}$$

so that

$$u/U_\infty = 2(\log\ 2/\pi)^{1/2}C_D^{1/2}(X/c)^{-1/2}\exp(-\log\ 2\ Y^2/b_{1/2}^2) \tag{6}$$

We also consider a semiempirical wake model described by Reynolds,[11] and referred to here as the Reynolds wake model, who used a substantial amount of wake data on isolated airfoils, cascades, and rotors to derive correlations for the development of the wake with downstream distance. The model appears to be the same as that used in Topol's[1] prediction scheme. Reynolds found that the wake profile was well represented by a Gaussian, although his model differed from that in Eqs. (3) and (6) in that the wake width scaled on $C_D^{3/4}$ instead of $C_D^{1/2}$ and the defect velocity on $C_D^{1/4}$ instead of $C_D^{1/2}$.

It is now assumed that the wake develops relatively slowly with downstream distance and a new reference system (x, y) is considered, in which the original system (X, Y) has been rotated through an angle α; x is thus measured parallel to the engine axis. The streamwise distance X and normal distance Y are related to x and y by $X = x\cos\alpha + y\sin\alpha$ and $Y = -x\sin\alpha + y\cos\alpha$, so that in the wake where $Y/c \ll 1$ we can put $X \sim x/\cos\alpha$. The wake width b will be assumed to be constant for X fixed and given by $b = b(X) = b(x/\cos\alpha - X_0)$.

After a little manipulation,[12] the wake velocity harmonics can be written in the form

$$u_n/U_\infty = -(\cos\alpha,\ \sin\alpha)cC_D/(2s\cos\alpha) \times \exp(-i2\pi n\tan\alpha\ x/s)G(k_b) \tag{7}$$

where $G(k_b)$ is a normalized Fourier coefficient with $G(0) = 1$, and k_b is defined by

$$k_b = 2\pi nb/(s\cos\alpha) \tag{8}$$

For the Schlichting wake model the Fourier coefficient is given by[12]

$$G(k_b) = 40/(3k_b^4)\{(1 - \cos k_b - k_b\sin k_b) + (k_b^2/2)\sqrt{[\pi/(2k_b)]}C[\sqrt{(2k_b/\pi)}]\} \tag{9}$$

For the Reichardt wake model the normalized Fourier coefficients are obtained as

$$G(k_b) = \exp[-k_{b_{1/2}}^2/(4\ \log\ 2)] \tag{10}$$

where $k_{b_{1/2}} = 2\pi nb_{1/2}/(s\cos\alpha)$ is based on the wake width at half the defect velocity. A similar result is obtained for the semiempirical wake model of Reynolds that also has a Gaussian profile, although for that case the semiwake width will be different (larger for moderately or heavily loaded blades and smaller for lightly loaded blades). It is clear from Eq. (10) that the velocity harmonics will decay rapidly at high harmonics for the Reichardt wake and the Reynolds wake, with the rate of decay itself increasing with wake width. This rapid decay is because of the smoothness of the Gaussian profile. From Eq. (9), however, we see that the Schlichting wake harmonics decay only algebraically at high harmonics. In this case, though, it is clear from Eq. (1) that the wake profile is not perfectly smooth; the high Fourier harmonics are governed by the wake endpoints (unlike the Reynolds and Reichardt models the Schlichting wake has finite width), and by the kink (discontinuity in the second derivative) at the wake centerline, as is indicated by asymptotic analysis.[12] The harmonic decay rates will be discussed in conjunction with data shown next.

B. Comparisons with Data

The profiles predicted by each of the three methods are now compared with measurements. The test vehicle is a single-stream 15-in.-diam fan rig with a design speed of 21,343 rpm and a design pressure ratio of 1.4. All of the tests were conducted with 27-clappered rotor blades. A detailed discussion of the rig is given by Schwaller et al.[13] As part of a later test series some additional (limited) measurements were taken of the rotor wakes using hot-wire anemometry at an axial station two chord lengths downstream of the rotor. These hot-wire measurements of the wake defect velocities are felt to be accurate to within about 10%. The rotor section drag coefficients, needed as input to the wake models, were obtained from a standard Rolls–Royce, plc. throughflow calculation.

A sample comparison between measured data and the wake models is shown in Fig. 1 at 40% of design speed and at 45% annulus height. We note that the Schlichting and Reichardt models produce almost identical results, as might be expected

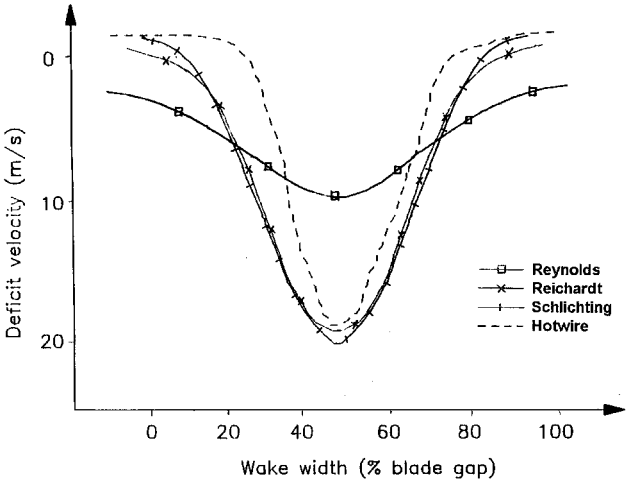

Fig. 1 Comparison of measured and predicted rotor wake deficit (40% design speed, 45% annulus height).

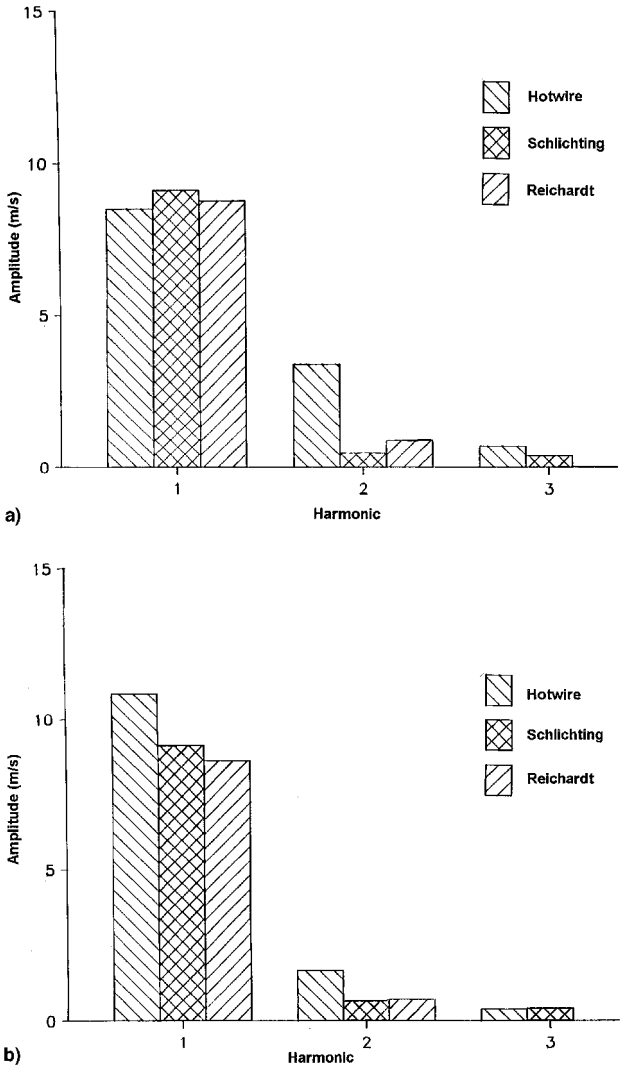

Fig. 2 Comparison of measured and predicted wake harmonics (40% design speed): a) 45 and b) 90% annulus height.

(cf., Fig. 24.5 of Schlichting[6]). These two models agree reasonably well with the measured wake profile and predict the centerline defect velocity accurately and the width to within about 70%. Since there is, clearly, some difference in measured and predicted wake profile areas, the discrepancy may be caused, in part, by some error in the calculation of drag coefficient, or by the assumption of locally two-dimensional flow, and not necessarily by any deficiency in the wake models. The semiempirical model of Reynolds[11] produces about half the defect velocity and twice the wake width of the classical models. These results seem to agree, qualitatively, with those of Topol,[1] who used, essentially, the same semiempirical wake model[14] and found that to get good agreement with measured data it was necessary to halve the wake width obtained from the model.

At this stage then, because of the poor agreement with measured data, the semiempirical Reynolds wake model is discarded. However, we note that the model was developed for lightly loaded blades with, of course, low drag coefficients. Indeed, since the centerline velocity of the Reynolds wake scales on $C_D^{1/4}$, it will become greater than that of the other two models, which scale on $C_D^{1/2}$, as C_D decreases. We estimate that the Reynolds and Reichardt models will be virtually identical when $C_D = 0.007$; in such a low drag regime the Reynolds model would be expected to perform extremely well.

In Figs. 2a and 2b we show the harmonic decay of the measured and predicted wake profiles at 45 and 90% blade height, respectively, for the first three blade passage harmonics. At the first harmonic there is reasonable agreement between the measured wake and both of the classical wake models, particularly at 45% blade height. At the second harmonic the measured wake amplitude is significantly higher than both of the classical wake amplitudes, with the Reichardt model producing a level slightly higher than that produced by the Schlichting model. At the third harmonic the measured wake agrees reasonably well with the Schlichting wake, but the Reichardt wake is negligible. The Reichardt wake, of course, decays exponentially with harmonic and we would expect it to become negligible at around the third harmonic, although it is important to note that the measured harmonics are not negligible there. However, in spite of this exponential decay, the Reichardt wake level is higher than the Schlichting wake level at second harmonic. To understand the reasons for these harmonic variations the Fourier coefficients will be examined in more detail.

Figure 3 shows a comparison of the normalized Fourier coefficients $G(k_b)$ for the three wake models including the Reynolds semiempirical model. {Note that to obtain a precise comparison, the Reichardt and Reynolds models have been calculated in terms of an effective full-wake semiwidth b, based on the Schlichting wake semiwidth, rather than the half-wake semiwidth $b_{1/2}$. From Eqs. (2), (3), and (8) $k_b = 4\beta\sqrt{10}k_{b_{1/2}}$ so that, for the Reichardt model, Eq. (10) is replaced by $G(k_b) = \exp[-k_b^2/(640\beta^2 \log 2)]$. In addition, for the fan under consideration, the Reynolds wake width is approximately twice that of the Schlichting and Reichardt models. For the Reynolds model, then, we use $G(k_b) = \exp[-k_b^2/(160\beta^2 \log 2)]$.} The results show the anticipated rapid decay of the Reichardt and Reynolds harmonics. The Fourier coefficients of the Schlichting wake, however, decay much more slowly (algebraically), and it is clear that there is a significant dip in the values of the Schlichting coefficients at moderate values of k_b, where the values are lower than those of the Reichardt coefficients. Since the flow exit angle of the rotor blade increases with radius, because of increasing blade speed, the wake width, as seen by the stator leading edge, will increase with radius because of 1) the effect of the relative flow angle, which produces an effective wake width $b/\cos\alpha$; 2) the increased distance $x = g/\cos\alpha$, where g is the axial interrow gap that the wake has to travel, thus leading to greater wake spreading; and 3) radial variations in section drag. This variation in wake width leads to variations in wake wave number and can be perceived as producing some smoothing of the results. Nonetheless, it is clear from Figs. 2 and 3 that the dip in the Fourier coefficients of the Schlichting wake is significant and will affect the noise radiation results. The experimental

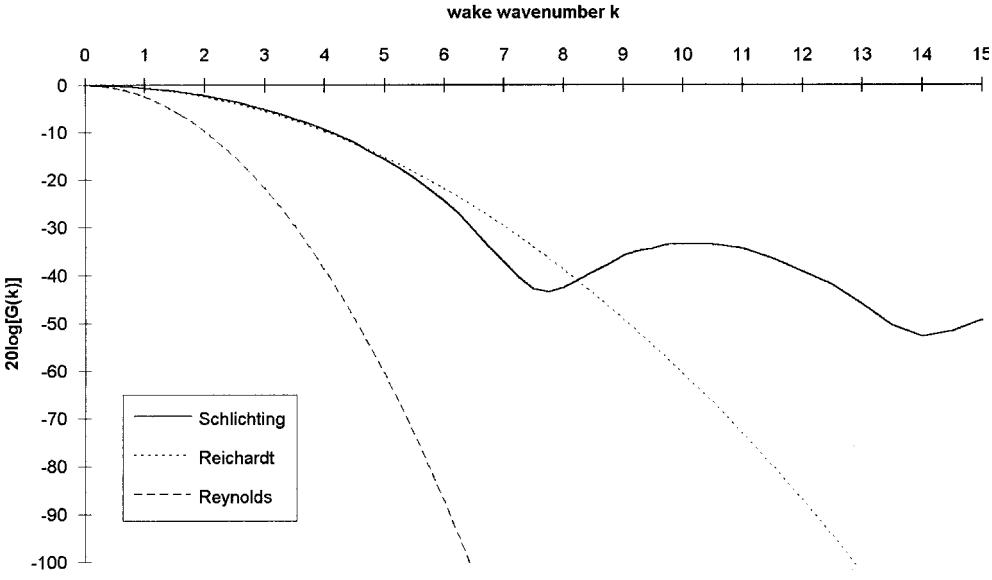

Fig. 3 Predictions of the normalized Fourier coefficients.

results, though, show no dip at second harmonic and no significant drop in level at third harmonic, where the measurements agree with the Schlichting wake prediction, suggesting that the envelope decay of the Schlichting wake harmonics is reasonable, but that the oscillations are not. There will be some further discussion of the harmonic decay rates in Secs. V.A and V.B in relation to the measured and predicted far-field noise.

III. Blade Response

In previous calculations[2,12,15] of blade response on open rotors, the present author used an analytical scheme for interactions between fixed harmonics of an incident velocity field and an isolated semi-infinite flat plate in compressible flow (different response functions are obtained for upstream and downstream calculations and for wake and potential interactions). Note that the compressible flow assumption is essential for all aerodynamic interactions, of practical interest, between disturbances and a rotating blade row since the blade relative Mach numbers are, generally, in the high subsonic regime. That open-rotor scheme is valid at moderate–high frequency for relatively thin and lightly cambered blades on blade rows that have high space–chord ratios. The two-dimensional response calculations, used in the scheme, are applied to three-dimensional blade rows using a simple strip theory assumption.

To extend the scheme for application to blade rows with low space–chord ratios it is important that cascade effects are included in the response calculation module: these cascade effects represent the modification of the unsteady flow about an individual blade by the adjacent (and nearby) blades on the same row. In this paper it is assumed that the coupling effect of the cascade is the dominant factor and that the effects of blade thickness and camber can be neglected to a first approximation. In addition it is assumed that the strip theory assumption is still valid. It is emphasized, however, that blade thickness, camber, and three-dimensional response effects can all be included within the general framework described here if required.

Consequently, the blade response, to a fixed incoming velocity harmonic, will be calculated for a two-dimensional linear cascade of flat plates at zero incidence to a compressible subsonic flow. The scheme LINSUB, developed by Whitehead[16,17] and based on the analysis of Smith,[18] is ideal for these purposes and has been incorporated, as a callable subroutine, into the general prediction scheme. (Note that LINSUB is similar to the numerical scheme for stator response developed by Ventres et al.[19] and used by Topol[1] for predictions of rotor wake–stator interaction noise.) The code is used to calculate the chordwise unsteady pressure distributions at a number of radial heights. Values at intermediate spanwise or chordwise stations are obtained using a standard bicubic spline routine.

The incident gust, or velocity harmonic, is a complex quantity with its amplitude and phase determined separately for each radial station and based on the local distance that the wake travels relative to the upstream blade row, i.e., parallel to the exit relative flow angle of the upstream blade row. The original open rotor calculation scheme has been updated to include the effects of interrow swirl velocities, thus allowing us to determine accurately the propagation direction of the wake, and the leading-edge stagger angles of the downstream blades. (Here it has been assumed, as in previous open rotor calculations, that the aerodynamic interactions are leading-edge dominated. The cascade stagger angle used in the LINSUB calculations is thus taken to be the leading-edge angle.) Note that, since the interaction calculations are applied on the basis of strip theory, and since the general framework is the same as that previously used for propfans, we can include the radial dephasing effects of blade sweep in the calculations. The frequency of the aerodynamic interaction (which is not necessarily the same as the frequency of the radiated sound field) is, of course, determined in the frame of reference of the downstream row. Complete details of the relevant coordinate transformations are given in Refs. 2 and 12.

IV. Noise Radiation

The third module in the prediction scheme is the model for the far-field radiation caused by the unsteady blade forces. Topol[1] applied a Green's function approach to a series of dipoles in an infinite length, constant area, annular duct to calculate the amplitudes, phases and power levels of each cut-on mode in the duct. There each upstream and downstream propagating mode was represented by a distinct circumferential order and a distinct radial order.

Here the approach is much simpler. It is supposed that at the moderate–high frequencies of interest, the effect of the (hardwalled) duct is merely to modify the directivity, but not the power, of the radiated sound field: all of the upstream propagating modes in the duct are assumed to suffer negligible reflection from the intake lip. In addition, the effects of transmission of the sound field through an upstream blade row are neglected (at least in the present paper), although such effects can be important and can lead not just to the attenuation of an incident circumferential mode, but also to the scattering of a mode into other modes and, if the blade row is rotating, into

other frequencies. Consequently, for the purposes of calculating the radiated sound power, the duct can be removed completely and the ducted fan treated as an open rotor. Of course, for an open rotor there is, formally, no definition of cut on or cut off. However, in the frequency domain approach used here there is a very strong analogy, particularly at moderate–high frequencies, between cut off in ducts and poor radiation efficiency on open rotors with modes that would be cut off at a given frequency in ducts having very low (in most case exponentially small) radiation efficiency.[2]

There are a number of advantages in using an open rotor calculation. Firstly, for open rotors, the required sound field is calculated using the simple free space Green's function, rather than the ducted Green's function for an annular duct that leads to the introduction of cylinder functions. Secondly, the open rotor approach leads to the production of only circumferential order modes, whereas the ducted rotor approach, in which the duct wall boundary condition must be satisfied, leads to the generation of a number of radial orders for each circumferential order mode, and each of these radial orders must be considered, and computed, separately. Thirdly, the far-field sound pressure levels can be determined immediately without the need to carry out an intermediate duct diffraction calculation. Although the aim here is just to determine the radiated sound power levels, it is noted that for each cut-on mode there are a number of nil-shielding directions, corresponding to mode-ray angles, in which the duct has no effect whatsoever[20] and the open rotor and ducted rotor results are identical. At higher frequencies, therefore, when a number of circumferential order modes are cut on and there are a large number of nil-shielding directions, the open rotor approach should produce a reasonable prediction of the radiated directivity pattern, as well as the total sound power. Indeed, the scheme described here can be extended easily, via Chapman's open-to-ducted rotor transfer function,[20] to account for the effect of the duct on the radiated field.

The radiation formulas used in the present calculations, then, are precisely those used in previous propfan calculations[2,12,21]; although the blade unsteady forces, needed as input to the radiation calculations, are calculated using the LINSUB approach outlined in the previous section. The open rotor approach thus has the additional advantage of being able, if required, to utilize the asymptotic approximations described in detail by Parry[12] and Parry and Crighton.[2] Such asymptotic techniques are invaluable when a large number of interaction tones (or modes) are generated in the audible frequency range. The essence of the asymptotic approach is to show that, for each interaction component, the far-field radiation is dominated by the radiation from a single blade radius, termed the Mach radius, thus allowing the radial integration (i.e., one of the integrals over the source region) to be calculated analytically. At the Mach radius, though, the local two-dimensional calculation is carried out precisely.

Note in the present scheme that, when multiple circumferential modes are generated at the same frequency, the solution is obtained as a simple rms summation in each far-field direction. Any particular effects arising from mode–mode interference will, therefore, not be captured. In principle, these interference effects can be included in an open rotor scheme, within the limitations described by Chapman,[20] but they have been neglected in the present approach, partly for simplicity and partly because it was felt that the effects of rotor blockage would be more important and would also result in phase changes.

V. Far-Field Noise—Theory vs Data

A. Previous Validation

Having outlined the framework of the prediction scheme in Secs. II–IV, we will now consider the radiated sound field and show comparisons between measurements and predictions. The modular prediction scheme, developed as an extension to an open rotor scheme, has already been validated against measured data from a contrarotating propeller.[2] There it was found that the first few aerodynamic interaction tones were dominated by potential field interactions (both upstream and downstream) rather than by wake interactions, and that excellent predictions could be made not only of the absolute level of the far-field sound but also of the detailed directivity pattern. Here the intention is to extend the validation process using two additional sets of data relating to completely different configurations. Both of these configurations are ducted and, from the discussion in the previous section, it seems logical, at least at this stage, to restrict the comparison to sound power levels rather than to detailed directivities, partly because the open rotor approach neglects the effect of diffraction by the duct, and partly because the standard flanged or unflanged cylindrical duct diffraction calculations are invalid for the bellmouth intakes used on the rigs.

B. Conventional Single-Stream Fan

The first configuration is the conventional single-stream fan rig described, briefly, in Sec. II, and in more detail by Schwaller et al.[13] The 27-bladed fan was tested with a number of different vane/blade ratios. Here, results and the corresponding theoretical noise predictions are shown for three cases: 1) a 32-vaned stator with a cut-on blade passing frequency tone, 2) a 48-vaned stator for which the blade passage tone is cut off (at the fan speed considered here), and 3) a 56-vaned stator that also has a cut-off blade passing frequency tone. For each of these cases we consider the first three harmonics of blade passing frequency and show the measured and predicted forward-arc sound power levels. The measured data shown here were acquired in an anechoic test facility and are felt to be accurate to within around 1 dB. Predictions are obtained using both the Schlichting and Reichardt classical wake models. All measured and predicted noise levels were obtained for a rotor–stator spacing of two rotor chords. Note that the induct mode detection results[13] show clearly that the noise is dominated by rotor–stator interaction and not by intake distortion, as indicated by a difference of more than 10 dB between cut-on and cut-off blade passing frequency tone levels.

The results for the 32-, 48-, and 56-vane cases are shown in Figs. 4–6, respectively, where, for the 48- and 56-vane cases, the cut-off first harmonic has been excluded. The figures show that the predictions using the Reichardt wake model decay too rapidly at higher frequencies, resulting in a consistent underprediction of 15–20 dB at third harmonic. In addition, we see that despite this rapid harmonic decay, the Reichardt

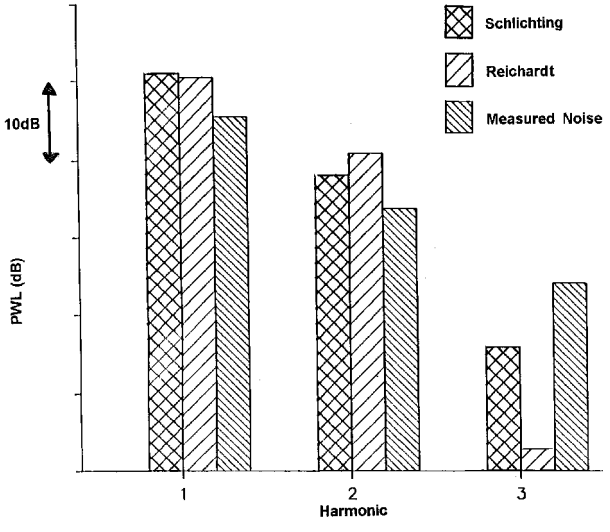

Fig. 4 Comparison of measured and predicted far-field tone levels (40% speed, 32 vanes).

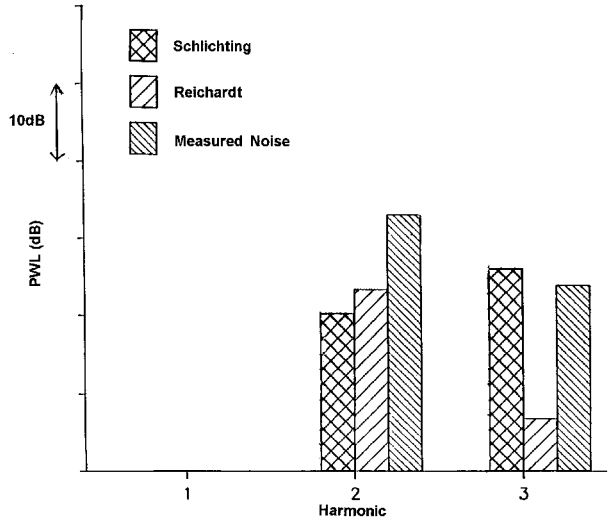

Fig. 5 Comparison of measured and predicted far-field tone levels (40% speed, 48 vanes).

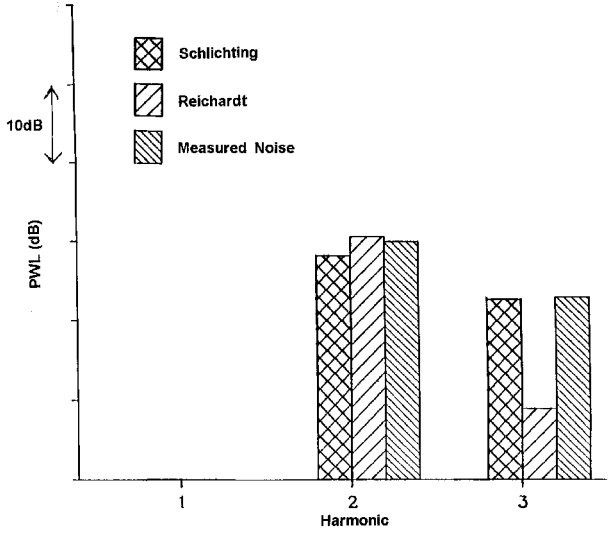

Fig. 6 Comparison of measured and predicted far-field tone levels (40% speed, 56 vanes).

prediction always lies above the Schlichting prediction at second harmonic, showing, from Fig. 3, that the wake wave numbers, corresponding to the second harmonic of the radiated sound, lie in the region of the dip in the Schlichting wake coefficients and that radial integration has not smoothed out the effects of the dip. In this region (i.e., at second harmonic) the differences between the two noise predictions are not particularly large (less than 3 dB) compared to the differences between measurement and prediction, and the wake velocity harmonic results in Figs. 2a and 2b, discussed in Sec. II, showed that the dip in the Schlichting wake coefficients and the exponential decay of the Reichardt wake coefficients leads to an underprediction by both models, at the second harmonic, of at least 50% (dependent on radius), corresponding to more than 6 dB in the radiated sound field. Since the Reichardt prediction is too low at both second and third harmonics, the remainder of this section concentrates solely on the Schlichting prediction.

In spite of this expected underprediction at second harmonic, Figs. 4–6 show that the Schlichting model, in fact, overpredicts the sound power by around 5 dB at second harmonic in the 32-vane case and is in close agreement (within 2 dB) with the measurements at second harmonic in the 56-vane case. In addition, note that the data are overpredicted by around 5 dB at first harmonic in the 32-vane case and by around 3 dB at third harmonic in the 48-vane case. Each of these four cases, however, corresponds to aerodynamic interactions that produce a single contrarotating mode ($m = -10$ at second harmonic in the 32-vane case, $m = -2$ at second harmonic in the 56-vane case, $m = -5$ at first harmonic in the 32-vane case, and $m = -15$ at third harmonic in the 48-vane case), and we would expect such modes to suffer strong rotor blockage effects. Mode detection results[13] show that reductions in sound power level of the order of 10 dB are typical, although the precise blockage will, of course, vary with frequency and mode number.

There are three other tones to be considered in Figs. 4–6. The second harmonic in the 48-vane case corresponds to a single corotating mode $m = 6$, which would be expected to suffer little, if any, blockage on passage through the rotor and the underprediction of around 10 dB is broadly consistent with the expected dip at second harmonic. Finally, the third harmonics in the 32- and 56-vane cases correspond to aerodynamic interactions that produce both a corotating and a contrarotating mode ($m = 17$ and -15 in the 32-vane case, and $m = 25$ and $m = -31$ in the 56-vane case) and, consequently, we cannot be certain what reductions there should be in predicted sound power, if any, to account for the effects of rotor blockage. There is excellent agreement between measurement and prediction in the 56-vane case, but the prediction is around 7–8 dB below the measurement in the 32-vane case. The reasons for the underprediction of sound power are, at present, unclear, although it is possible that the low level is because of an underprediction of the wake velocity harmonics at these high frequencies (note that the comparison between measured and predicted wake harmonics in Fig. 2 suggests that any underprediction is confined to low–moderate radial heights) or to frequency scattering of the first and/or second harmonics off the rotor that can result in enhancement of the higher harmonics (see Topol et al.[22]), or to the mode–mode interference effects.

In general, the results show that far-field sound power levels can be predicted to within 10 dB, neglecting rotor blockage effects. It is clear that although the present best wake model (Schlichting) produces reasonable (envelope) harmonic decay at high frequencies compared to the Reichardt wake model. It still needs some modification: firstly, to remove the oscillations that result in a dip at second harmonic that is not present in the measured data and, secondly, to improve slightly the high-frequency (envelope) decay rate. It is also clear that, since rotor blockage effects can be significant, the prediction scheme should include an additional module to account for blade row attenuation.

C. Contrafan

The second configuration is a one-sixth scale model of the fans and bypass duct of the Rolls-Royce, plc. RB529 contrafan engine. The rig was tested in the German Dutch anechoic wind tunnel DNW at tunnel speeds up to Mach 0.22. Once again the measured noise levels are expected to be accurate to within about 1 dB. Complete details of the configuration of the rig and the noise test series are described by Henshaw.[23] The rig is shown in Fig. 7. It has a set of five front inlet struts, two contrarotating rotors with 24 blades on the front rotor and 19 blades on the rear rotor, and a set of nine rear exit struts. For the purposes of noise prediction only the aerodynamic interactions between adjacent blade rows are considered. There are thus three separate sets of predictions that must be made: 1) the stator–rotor aerodynamic interaction between the inlet struts and the front rotor producing modes $m = 24n_1 - 5k$ at frequencies $f = 24n_1E_1$, where n_1 and k are integers and E_1 is the front rotor shaft frequency; 2) the rotor–rotor aerodynamic interaction between the front and rear rotors producing modes $m = 24n_1 - 19n_2$ at frequencies $f = 24n_1E_1 + 19n_2E_2$, where n_2 is an integer and E_2 is the shaft frequency of the rear row;

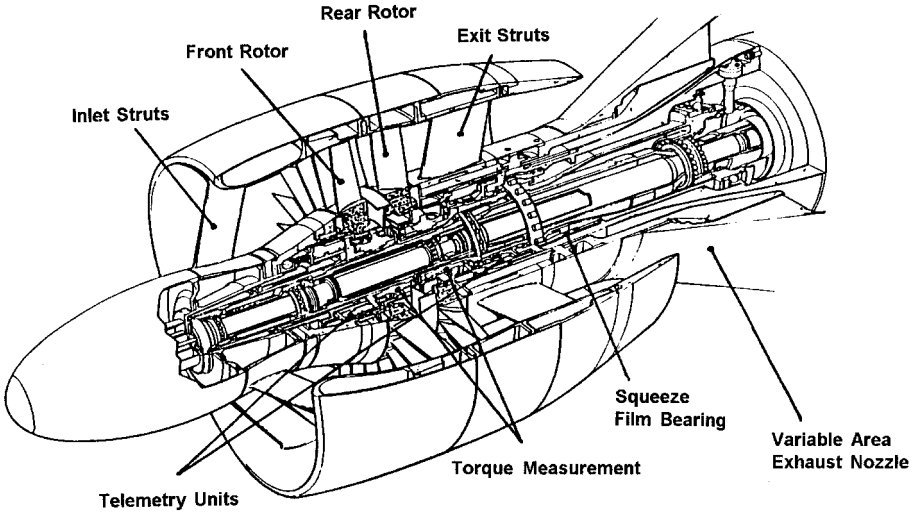

Fig. 7 Contrarotating ducted fan rig 141.

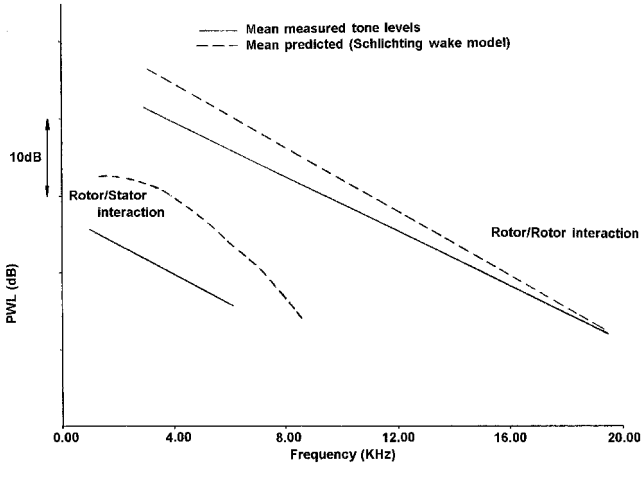

Fig. 8 Comparison of measured and predicted tone levels for contrarotating ducted fan rig 141 (low spacing, 60% design speed).

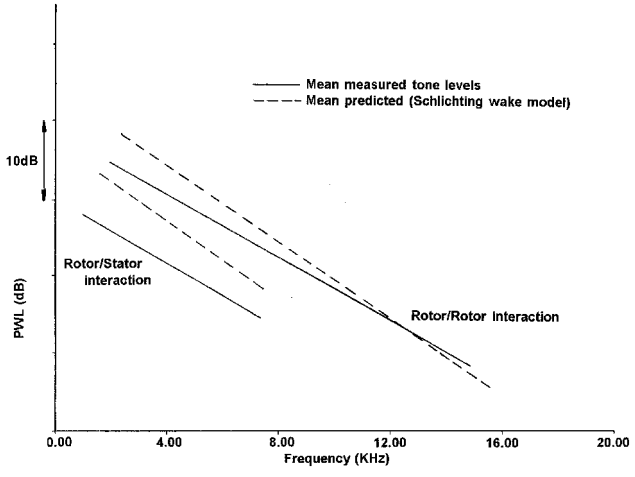

Fig. 9 Comparison of measured and predicted tone levels for contrarotating ducted fan rig 141 (high spacing, 60% design speed).

and 3) the rotor–stator interaction between the rear rotor and the rear exit struts producing modes $m = -19n_2 + 9k$ (relative to the front rotor) at frequencies $f = 19n_2E_2$. Note that, because of the difference in the front and rear row blade numbers, the three sets of aerodynamic interactions all occur at different frequencies: at each harmonic of the front or rear rotor passage frequency there are a number of spining modes; each sum tone, however, generated by the rotor–rotor aerodynamic interaction produces a single mode. Results at 60% of fan design speed and at two separate rotor–rotor spacings are considered. The inlet struts-front rotor spacing and rear rotor-exit struts spacing are maintained constant. In the prediction method the Reichardt wake model is discarded because the resultant wake Fourier harmonics decay too rapidly at high frequency, as was shown in Sec. V.B, and just the Schlichting wake model is used.

For this configuration the far-field sound power spectrum consists of a profusion of tones,[23] many of which (particularly the rotor–rotor and rotor-rear strut interaction tones) will be affected by frequency scattering. To simplify the presentation of the results a best curve has been fitted to both the data and the predictions and the combination tones (from rotor–rotor interactions) and the front or rear rotor blade passage tones (from inlet strut-front rotor or rear rotor-exit strut interactions) have been considered separately. Note that, because of the high spacing between the inlet struts and the front rotor, the rear rotor blade passage tones are much higher than the front rotor blade passage tones. Consequently, although the inlet strut-front rotor interactions are included in the measurements and predictions, the combined results will be referred to as the rotor–stator interaction.

The results are shown in Figs. 8 and 9 for the low- and high-spacing cases, respectively. The first and most important point to note is that the mean measurements and predictions (i.e., measured and predicted curvefits) of sound power level (PWL) agree to within 10 dB for both rotor–rotor spacings, for both rotor–rotor and rotor–stator interactions, and at all frequencies (20 kHz at model scale corresponds to 3 kHz at full scale; this frequency range covers around the first 10 combination harmonics). In addition, note that agreement between measurement and prediction is better for rotor–rotor interactions than for rotor–stator interactions, it is better at higher frequencies, and it is better at higher spacings. It appears, therefore (at least initially), that agreement between theory and data improves with increasing k_b: wake passage frequency is higher for rotor–rotor interaction than for rotor–stator interaction leading to higher k_b; k_b increases, clearly, with harmonic or frequency; and, at higher spacings, b, and therefore k_b, is greater. Neglecting blade row attenuation effects, one would expect the agreement between measurement and prediction to be closest at low wake wave numbers where the precise details of the wake profile become unimportant (as shown by the close agreement between the three sets of wake coefficient predictions in Fig. 3). Consequently, it is possible that there is some

error in the derived drag coefficient that is used in the wake model. Such an error could, of course, be calibrated out of the results. There is no need to undertake that calibration here since any error, once corrected, would clearly lead to good agreement at low frequencies and an underprediction at higher frequencies that increases monotonically with wake wave number.

It is concluded that the prediction scheme, in its present form, can generally predict far-field sound power levels to within 10-dB for rotor–rotor, rotor–stator, and stator–rotor interactions. The results are also consistent with those from the single-stream fan rig and suggest that, to obtain an improved level of agreement between theory and data across a broad range of frequencies, some modifications to the Schlichting wake model are required, and blade row attenuation effects need to be included in the scheme.

VI. Concluding Remarks

A previously developed prediction scheme for noise generated by contrarotating propellers has been extended, with a minimum amount of modification, to predict the sound power levels radiated from many-bladed configurations. Three wake models were considered, two of which are classical and one of which is semiempirical. It was found that, at least for the configurations examined here, both of the classical models were much better than the semiempirical model, but that only one model[8] was reasonable at high frequencies. The effects of high blade number on blade unsteady response have been accounted for by the use of the standard flat plate cascade routine LINSUB, and acoustic radiation to the far field has been calculated using an open rotor approach.

The theoretical method has already been validated, in detail, against previous flight tests on a contrarotating propeller[2]; here we have also shown comparisons with measurements at the first three harmonics of blade passing frequency on a conventional single-stream fan rig, and with data from a ducted contrafan model up to around the tenth (combination) harmonic. In general, there is agreement between measurement and prediction, excluding the significant effects of rotor blockage, to well within 10 PWL dB for all cases and frequencies considered. It is clear that the level of agreement between theory and data can be improved by extending the prediction scheme to account for rotor blockage effects, and by making some modifications to the wake model. Consequently, a detailed package of work[24] is in progress that is aimed, in part, toward the acquisition of further wake and rotor blockage data necessary for validation of new wake and blade row attenuation modules.

Acknowledgments

The experimental data described in Secs. II and V were acquired with the support of the Department of Trade and Industry (Civil Aircraft Research and Demonstration Programme) through the Defence Evaluation Research Agency, Pyestock, England, UK. The author would like to thank his colleagues S. Gormley and P. Swann for assistance in collating and appraising the rig data, and the Directors of Rolls-Royce, plc. for permission to publish this paper.

References

[1]Topol, D. A., "Rotor Wake/Stator Interaction Noise — Predictions vs Data," *Journal of Aircraft*, Vol. 30, No. 5, 1993, pp. 728–735.

[2]Parry, A. B., and Crighton, D. G., "Theoretical Prediction of Counter-Rotating Propeller Noise," AIAA Paper 89-1141, July 1989.

[3]Majumdar, S., and Peake, N., "The Theory of Unsteady Distortion Noise for Fans," CEAS/AIAA Paper 95-023, June 1995.

[4]Majumdar, S., and Peake, N., "Three Dimensional Effects in Cascade-Gust Interaction," *Wave Motion*, Vol. 23, 1996, pp. 321–337.

[5]Crighton, D. G., "Asymptotic Methods for Turbomachinery Noise Prediction," AIAA Paper 95-002, June 1995.

[6]Schlichting, H., *Boundary Layer Theory*, McGraw–Hill, New York, 1955.

[7]Goldstein, S., *Modern Developments in Fluid Dynamics*, Clarendon, Oxford, England, UK, 1938; also Dover, New York, 1965.

[8]Schlichting, H., "Über das ebene Windschattenproblem," *Ingenieur Archiv*, Vol. 1, 1930, pp. 533–571.

[9]Reichardt, H., "Gesetzmäßigkeiten der freien Turbulenz," VDI-Forschungsheft 414, 1942.

[10]Görtler, H., "Berechnung von Aufgaben der freien Turbulenz auf Grund eines neuen Näherungsansatzes," *ZAMM*, Vol. 22, 1942, pp. 244–254.

[11]Reynolds, B. D., "Characteristics of the Wake of a Lightly Loaded Compressor or Fan Rotor," AIAA Paper 79-0550, Feb. 1979.

[12]Parry, A. B., "Theoretical Prediction of Counter-Rotating Propeller Noise," Ph.D. Dissertation, Dept. of Applied Mathematical Studies, Univ. of Leeds, Leeds, England, UK, 1988.

[13]Schwaller, P. J. G., Parry, A. B., Oliver, M. J., and Eccleston, A., "Farfield Measurements and Mode Analysis of the Effects of Vane/Blade Ratio on Fan Noise," AIAA Paper 84-2280, Oct. 1984.

[14]Reynolds, B. D., and Lakshminarayana, B., "Characteristics of Lightly Loaded Fan Rotor Blade Wakes," NASA CR-3188, Oct. 1979.

[15]Parry, A. B., "The Scattering of Velocity Fields by an Airfoil in Compressible Flow," *Inverse Problems and Imaging*, Longman Higher Education and Reference, Harlow, UK, 1992, pp. 127–154.

[16]Whitehead, D. S., "Vibration and Sound Generation in a Cascade of Flat Plates in Subsonic Flow," Cambridge Univ. Engineering Dept., Rept. CUED/A-Turbo/TR 15, Cambridge, England, UK, 1970.

[17]Whitehead, D. S., "Classical Two-Dimensional Methods," *AGARD Manual on Aeroelasticity in Axial Flow Turbomachinery Volume 1 Unsteady Turbomachinery Aerodynamics*, edited by M. F. Platzer and F. O. Carta, Vol. 1, AGARD-AG-298, 1987, Chap. 3.

[18]Smith, S. N., "Discrete Frequency Sound Generation in Axial Flow Turbomachines," Aeronautical Research Council, R&M 3709, March 1972.

[19]Ventres, C. S., Theobald, M. A., and Mark, W. D., "Turbofan Noise Generation," NASA CR-167952, Vols. 1 and 2, July 1982.

[20]Chapman, C. J., "Sound Radiation from a Cylindrical Duct. Part 2. Source Modelling, Nil-Shielding Directions, and the Open-to-Ducted Transfer Function," *Journal of Fluid Mechanics*, Vol. 313, 1995, pp. 367–380.

[21]Hanson, D. B., "Noise of Counter-Rotation Propellers," *Journal of Aircraft*, Vol. 22, No. 7, 1985, pp. 609–617.

[22]Topol, D. A., Holhubner, S. C., and Mathews, D. C., "A Reflection Mechanism for Aft Fan Tone Noise from Turbofan Engines," AIAA Paper 87-2699, Oct. 1987.

[23]Henshaw, D. G., "An Experimental Evaluation of Prediction Methods for Contrafans," AIAA Paper 92-02-135, May 1992.

[24]Henshaw, D. G., "Aeroacoustic Methods for Fan Noise Prediction and Control (FANPAC)," 2nd Aerodays European Community Aeronautics Conf., Naples, Italy, Oct. 1993.